

Defect formation and local gauge invariance

M. Hindmarsh and A. Rajantie

Centre for Theoretical Physics, University of Sussex, Falmer, Brighton BN1 9QJ, U. K.
(October 28, 2018)

We propose a new mechanism for formation of topological defects in a U(1) model with a local gauge symmetry. This mechanism leads to definite predictions, which are qualitatively different from those of the Kibble-Zurek mechanism of global theories. We confirm these predictions in numerical simulations, and they can also be tested in superconductor experiments. We believe that the mechanism generalizes to more complicated theories.

PACS numbers: 11.15.Ex, 11.27.+d, 74.60.Ge

SUSX-TH-00-012

hep-ph/0007361

When a global symmetry is spontaneously broken in a phase transition, it is generally accepted that the formation of topological defects is well described by the Kibble-Zurek (KZ) scenario [1,2]. As the transition takes place in a finite time, the correlation length of the order parameter cannot keep up with its equilibrium value, which diverges at the transition point. The maximum correlation length reached determines the average distance of the defects in the final state [1], and it can be estimated from the critical dynamics of the theory [2]. This scenario has been tested in many numerical simulations [3,4] and in experiments with ^3He [5] and ^4He [6]. Although the experimental results for ^4He are in disagreement with the theory, the general picture is believed to be correct.

However, in theories where the relevant symmetry is a local gauge invariance, e.g. in superconductors or in cosmology [7], the validity of the KZ scenario has been questioned [8], although lattice simulations [9] have found compatible results. Evidence that the KZ scenario might not work in these cases has been provided by recent experiments on YBCO superconductors [10]. Instead of detecting individual vortices, the authors measured the total net flux through the whole system, and found it to be zero within the accuracy of the experimental setup, in contradiction with predictions of the KZ scenario.

The purpose of this letter is to suggest a simple and intuitive picture for defect formation in theories with local gauge symmetries. This picture is quite different from the KZ scenario and leads to definite predictions, which we have confirmed in numerical simulations. Furthermore, they can also be tested in superconductor experiments.

Let us first review the KZ picture for the global case and consider for simplicity a U(1) symmetric field theory in D spatial dimensions. In the broken phase, the vacuum manifold is topologically a circle and the topological defects are therefore vortices with dimensionality $D - 2$. The Hamiltonian contains a gradient term $|\vec{\nabla}\phi|^2$, where $\phi = v \exp(i\theta)$ is the order parameter field. Deep in the broken phase, the gradient term implies that $\vec{\nabla}\theta \approx 0$ in equilibrium. Thus the phase angle is correlated at infinitely long distances, but since it takes an infinitely long time for the system to achieve that, after the transition θ will be approximately constant only inside domains of

size $\hat{\xi}$, given by the maximum correlation length reached during the transition, and its value will be uncorrelated between these domains [1]. Since vortices are characterized by a non-zero change of θ around a closed loop, they are formed where three domains meet with a probability that is independent of the size of the domains. Consequently, the final vortex number in the global case behaves as $N \sim \hat{\xi}^{-2}$. The value of $\hat{\xi}$ can be estimated from the critical slowing down of the dynamics during the transition [2].

If the symmetry is local, there is another, competing mechanism, which dominates if the transition is sufficiently slow. In the temporal gauge $A_0 = 0$, the Hamiltonian for a relativistic gauged U(1) scalar field theory in three spatial dimensions is

$$H = \int d^3x \left[\frac{1}{2} \vec{E}^2 + \frac{1}{2} \vec{B}^2 + |\Pi|^2 + |\vec{D}\phi|^2 + V(\phi) \right], \quad (1)$$

where $\Pi = \partial_0\phi$ is the canonical momentum, $\vec{E} = -\partial_0\vec{A}$ and $\vec{B} = \vec{\nabla} \times \vec{A}$ the electric and magnetic field strengths, and $V(\phi)$ the potential of the scalar field. The corresponding equations of motion are

$$\begin{aligned} \partial_0^2\phi &= \vec{D}^2\phi - V'(\phi), \\ \partial_0\vec{E} &= \vec{\nabla} \times \vec{B} + 2e\text{Im}\phi^*\vec{D}\phi, \\ \vec{\nabla} \cdot \vec{E} &= 2e\text{Im}\phi^*\partial_0\phi. \end{aligned} \quad (2)$$

(Note that we use units with $k_B = \hbar = c = \mu_0 = 1$.) More generally, we will consider the analogous system in D spatial dimensions. Because the gradient has been replaced by a covariant derivative $\vec{D}\phi = \vec{\nabla}\phi + ie\vec{A}\phi$, the energy is minimized in the broken phase if $\vec{\nabla}\theta \approx -e\vec{A}$. In the presence of a magnetic flux, this condition cannot be satisfied everywhere and frustrations, vortices, are formed. Although the magnetic flux is zero on the average, the thermal fluctuations give it a non-zero variance. When the system enters the broken phase, it tries to rearrange the field configuration to minimize the magnetic flux and the energy associated with it. Because of the finite time available, this is not possible for the fluctuations with the longest wavelengths and they freeze in their initial form, but at shorter distances the fluctuations of the magnetic flux are smoothed out. Therefore,

immediately after the transition, before the flux is localized into vortices, its configuration consists of domains inside which it is approximately uniform and which have some characteristic size $\hat{\xi}$.

If we calculate the winding number around a curve C , which encircles one of the domains discussed above, it typically does not vanish, but instead

$$n_C \equiv \frac{1}{2\pi} \int_C d\vec{r} \cdot \vec{\nabla} \theta \approx -\frac{e}{2\pi} \int_C d\vec{r} \cdot \vec{A} \equiv -\frac{e}{2\pi} \Phi_C, \quad (3)$$

where Φ_C is the magnetic flux through the curve C . Because the flux rearrangements at the transition were only able to change its distribution inside the domain, Φ_C has the same value it had in the symmetric phase. We can estimate it in the standard way by calculating the energy $E(\Phi_C)$ associated with the flux. Inside the domains, the flux is uniform and therefore

$$E(\Phi_C) \approx \hat{\xi}^D \left(\frac{\Phi_C}{\hat{\xi}^2} \right)^2 = \hat{\xi}^{D-4} \Phi_C^2. \quad (4)$$

Requiring $E(\Phi_C) \approx T$ gives the typical value of the flux

$$\Phi_C \approx T^{1/2} \hat{\xi}^{2-D/2}. \quad (5)$$

Using Eqs. (3) and (5), we can now estimate the area density of vortices after the transition. Suppose we have in our D -dimensional space a surface of area A , then it is split into $\sim A \hat{\xi}^{-2}$ domains in the transition. Each domain contains $N_0 \approx (e/2\pi) \Phi_C$ vortices, and we will assume that $N_0 \gtrsim 1$. Then, the total number of vortices piercing the surface per unit area is

$$N/A \approx \frac{e}{2\pi} T^{1/2} \hat{\xi}^{-D/2}. \quad (6)$$

In particular, at $D = 2$, $N \sim \hat{\xi}^{-1}$.

In addition, vortices will also be formed by a variant of the KZ mechanism. Initially, these vortices behave like global vortices, but eventually a quantum of magnetic flux is generated inside each of them, making them truly local vortices. However, the KZ mechanism is only important if the transition is very rapid or the temperature very low, i.e. $N_0 \lesssim 1$. Thus we will neglect it in the following.

At $D = 3$, the vortices formed inside the domains form a network at distances longer than $\hat{\xi}$, and in this network most vortices will be in the form of closed loops, which will quickly shrink into a point and disappear. Therefore it is useful to consider a border-line case between $D = 2$ and $D = 3$, where one of the dimensions L_z is very short. As long as $L_z \lesssim \hat{\xi}$, the vortices will wind around the short dimension rather than forming loops and therefore they will be stable. Now the domains have the form of a short cylinder, and the estimate (6) generalizes easily to this case, yielding

$$N/A \approx \frac{e}{2\pi} T^{1/2} L_z^{-1/2} \hat{\xi}^{-1} \sim L_z^{-1/2}. \quad (7)$$

The correlations between the vortices in the final state will also be different from those predicted by the KZ mechanism. Let us consider a system after the transition and assume that there is a vortex with a positive winding at point \vec{x} . In the KZ scenario, the distance to the nearest other vortex should be roughly $\hat{\xi}$. If we calculate the winding number $n_C(r)$ of a circular loop C of radius r centered at \vec{x} , it follows that at $r \lesssim \hat{\xi}$, the winding number is close to one. However, at distances $r \gtrsim \hat{\xi}$, the phase angle is independent of whether there is a vortex inside at \vec{x} or not, and therefore $n_C(r) = 0$. Thus, in the KZ scenario,

$$n_C(r) \approx \begin{cases} 1, & r \lesssim \hat{\xi}, \\ 0, & r \gtrsim \hat{\xi}. \end{cases} \quad (8)$$

Again, our case is very different. Inside a single domain, all vortices have the same sign, and $n_C(r)$ is therefore an increasing function of r at $r \lesssim \hat{\xi}$. At $r \gtrsim \hat{\xi}$, $n_C(r)$ gets contributions from different domains, and since they are all independent they average to zero and $n_C(r)$ becomes a constant. The behaviour in our scenario is therefore totally different from Eq. (8):

$$n_C(r) \approx \begin{cases} 1 + c_0 r^2, & r \lesssim \hat{\xi}, \\ c_1, & r \gtrsim \hat{\xi}, \end{cases} \quad (9)$$

where $c_0 \geq 0$ and $c_1 \geq 1$ are constants.

Finally, let us discuss the dependence of $\hat{\xi}$ on the ‘‘quench’’ timescale τ_Q , which parameterizes the rate at which the phase transition takes place. For definiteness, we consider the potential

$$V(\phi) = m^2(t) |\phi|^2 + \lambda |\phi|^4, \quad (10)$$

where the mass parameter is changed linearly across its critical value

$$m(t)^2 = m_c^2 - \delta m^2 \frac{t}{\tau_Q}. \quad (11)$$

In reality, m_c^2 is not equal to zero when thermal fluctuations are taken into account, but let us use the mean-field approximation in the following, in which case it is.

If we know the photon dispersion relation $\omega = \omega(k)$ at the transition point and its neighbourhood, we can estimate that a Fourier mode of wave number k_i falls out of equilibrium during the transition if the adiabaticity condition is not satisfied

$$\left| \frac{d\omega(k)}{dt} \right| > |\omega(k)|^2. \quad (12)$$

However, the calculation of the dispersion relation is beyond the scope of this letter, and we will instead only consider two simple special cases: the overdamped case (OD), where the dynamics is dominated by a k -independent damping rate γ , and the underdamped case (UD) with the free-field dispersion relation:

$$\omega = i\gamma^{-1}(k^2 + m_\gamma^2) \text{ (OD)}, \quad (k^2 + m_\gamma^2)^{1/2} \text{ (UD)}. \quad (13)$$

These same special cases have been discussed in the context of global theories in Ref. [4], but we stress that it is by no means clear that the dynamics is well described by either of these cases. Furthermore, we assume that the photon mass for the relevant modes behaves as $m_\gamma^2 \approx 2e^2|\phi|^2$, and that $|\phi|^2$ is given by its equilibrium value $|\phi|^2 = -m^2(t)/2\lambda \sim t/\tau_Q$.

Now, Eq. (12) tells us that the highest wave numbers that fall out of equilibrium behave as

$$\hat{k} \sim \tau_Q^{-1/4} \text{ (OD)}, \quad \tau_Q^{-1/3} \text{ (UD)}. \quad (14)$$

The domain size $\hat{\xi}$ is then simply given by $\hat{\xi} \approx 2\pi/\hat{k}$, and using Eq. (6), we can write down the dependence of the final vortex number on τ_Q in two dimensions as

$$N \sim \tau_Q^{-1/4} \text{ (OD)}, \quad \tau_Q^{-1/3} \text{ (UD)}. \quad (15)$$

In the KZ scenario, the analogous exponents are $-1/2$ and $-2/3$, respectively [4].

We carried out a set of numerical simulations using the equations of motion (2) to test the results in Eqs. (7), (9) and (15). Our coupling constants were $e = 0.3$ and $\lambda = 0.18$. Since $\lambda > e^2$, the transition is continuous, as in a Type II superconductor. We used periodic lattices of size $120 \times 120 \times L_z$, where $L_z = 5$ or 20 (in units where the lattice spacing is one). We prepared a set of initial conditions according to the thermal distribution $\exp(-H/T)$ at $T = 6$ using a hybrid Monte Carlo algorithm and followed the time evolution using a leap-frog algorithm with time step $\delta t = 0.05$, changing the mass parameter according to

$$m^2(t) = m_0^2 - \delta m^2 \left(\frac{4}{3\pi} \arctan \frac{t}{\tau_Q} + \frac{1}{3} \right). \quad (16)$$

Here $m_0^2 = -1.6$ is the initial value at $t = -\tau_Q$ when the quench begins and $\delta m^2 = 3.2$ was chosen in such a way that the transition takes place at $t \approx 0$. As in Eq. (11), the rate of change of m^2 is proportional to τ_Q , but in this form, we reach an equilibrium state at late times, which makes comparison of different quench rates easier. The details of the simulations will be discussed in Ref. [12].

In the final state, the vortices have only short-range interactions and therefore they freeze quickly into their final configuration. After that, at $t = \tau_Q + 400$, we located the vortices from the field configuration by measuring the gauge-invariant winding numbers of individual plaquettes [13] and connecting plaquettes with non-zero winding numbers into vortex lines. We then measured the total number of those vortex lines that wind around the short dimension of our lattice. The results are shown in Fig. 1 as a function of τ_Q . The results from the thinner lattice $L_z = 5$ have been divided by 2, because according to Eq. (7) the results from the two lattices should then

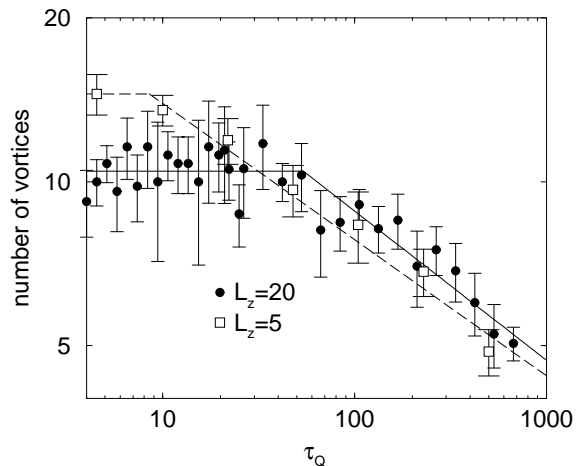


FIG. 1. The number of vortices in the final state as a function of τ_Q . The $L_z = 5$ data have been scaled by a factor of 1/2 in accordance with Eq. (7). The solid and dashed lines are the fits to Eq. (17) (see Table I) and correspond to the cases $L_z = 20$ and $L_z = 5$, respectively.

	c	τ_c	α	χ^2
$L_z = 5$	49.5 ± 2.6	8.5 ± 1.7	0.250 ± 0.013	6.73
$L_z = 20$	31.2 ± 6.7	54.1 ± 13.7	0.274 ± 0.039	12.09

TABLE I. Fit of the data to the functional form (17). Results from both simulations are compatible with the overdamped exponent $\alpha = 0.25$ (see Eq. (15)).

be on top of each other. Each datapoint is an average of ~ 20 runs starting from different initial configurations drawn from the thermal ensemble.

In slow transitions, the data agree very well with the predicted power-law behaviour. At $\tau_Q \lesssim 40-50$, the $L_z = 20$ data become independent of τ_Q , which suggests that $\hat{\xi} < L_z$, and part of the vortices have formed loops and do not contribute to the vortex count. We fitted the function

$$f(\tau_Q; c, \tau_c, \alpha) = \begin{cases} c\tau_c^{-\alpha}, & \tau_Q < \tau_c \\ c\tau_Q^{-\alpha}, & \tau_Q > \tau_c \end{cases} \quad (17)$$

into the data, and the results are given in Table I. Both cases agree with the overdamped prediction $\alpha = -0.25$. Moreover, the ratio of the results from $L_z = 5$ and $L_z = 20$ measured at, say, $\tau_Q = 100$, is 1.8 ± 0.2 , which is compatible with the value 2 predicted by Eq. (7).

Using our data, we can also perform a more quantitative check for Eq. (7) even without knowledge of the dynamics that determines $\hat{\xi}$, if we assume that $\hat{\xi} = L_z$ at the turning point in the $L_z = 20$ data. By substituting this into Eq. (7), we find that the number of vortices formed at $\tau_Q < \tau_c$ in the $L_z = 20$ case should be $N \approx 19$, which agrees within a factor of 2 with the numerical result.

We can also test Eq. (9) by measuring the net number of vortices inside a circle of radius r centered at a

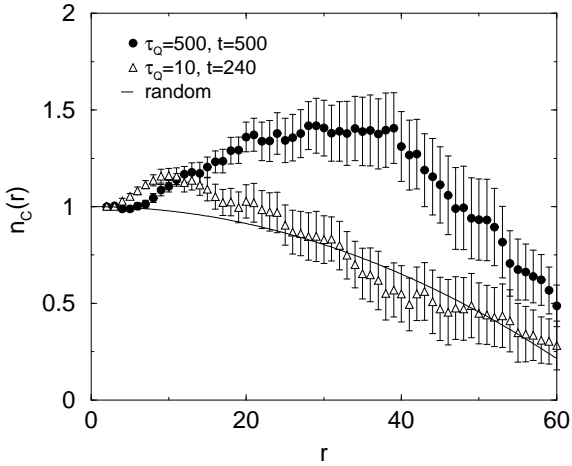


FIG. 2. The net number of vortices within distance r from a vortex with positive winding in a slow (circles) and a fast (triangles) quench on a thin lattice ($L_z = 5$). The dotted line is the corresponding curve for uncorrelated vortex-antivortex pairs. The fact that the data points are well above the random curve shows that there is a positive correlation between vortices at short distances.

vortex. The results for two different values of τ_Q with $L_z = 5$ are shown in Fig. 2, together with the benchmark curve $n_C = 1 - \pi r^2 A^{-1}$, which corresponds to a uniform random distribution of vortex-antivortex pairs and shows the effect of the finite system size. At short distances, the data points are significantly above this curve, which indicates a positive correlation between vortices, and at long distances, they follow the benchmark curve. Both of these results agree with Eq. (9) but differ from the KZ prediction (8).

Our results disagree with the simulations in Ref. [9], where the authors found an exponent α that was compatible with the global theory. We believe that the temperature used there, $T = 0.01$, was so low that practically all of the vortices were formed by the KZ mechanism.

Since our mechanism can only increase the number of vortices formed in a transition from that predicted by the KZ mechanism, it cannot explain the failure in Ref. [10] to find any total net magnetic flux when a superconductor film was quenched into the superconducting phase. However, the experiment does not rule it out either, because the vortices formed by the KZ mechanism might avoid detection by being expelled from the film before generating observable magnetic flux. The extra magnetic flux predicted by our mechanism is fairly small, because it can only change the flux distribution at short distances. The minimal energy for a configuration with a given value Φ of flux through the film is that of a magnetic dipole, $E_{\min} \approx \mu_0^{-1} A^{-1/2} \Phi^2$. Using the values $T = 90$ K and $A = 1$ cm², we find that the predicted number of flux quanta is

$$N \approx \frac{e}{\pi \hbar} (\mu_0 k_B T)^{1/2} A^{1/4} \approx 2, \quad (18)$$

which is below the resolution of the experiment. A similar estimate applies for a recent Josephson junction experiment [11], where $N \approx 7$ flux quanta were observed. In this case, the prediction of the KZ scenario is $N \approx 4$, and thus the experiment cannot decide between the two mechanisms. It seems that our scenario can only be confirmed by experiments in which not only the total flux but also the spatial distribution of the vortices can be measured.

To summarize, our numerical simulations confirm the results in Eqs. (7) and (9), which are independent of assumptions about the dispersion relation $\omega(k)$. Using the naive overdamped dispersion relation (13), we can also reproduce accurately the exponents α in Table I. This supports strongly the scenario presented in this letter.

AR was supported by PPARC and also partly by the University of Helsinki. Part of this work was conducted on the SGI Origin platform using COSMOS Consortium facilities, funded by HEFCE, PPARC and SGI. We acknowledge computing support from the Sussex High Performance Computing Initiative.

-
- [1] T.W.B. Kibble, *J. Phys.* **A9**, 1387 (1976).
 - [2] W.H. Zurek, *Nature* **317**, 505 (1985); *Phys. Rept.* **276**, 177 (1996) [cond-mat/9607135].
 - [3] P. Laguna and W.H. Zurek, *Phys. Rev. Lett.* **78**, 2519 (1997) [gr-qc/9607041]; N.D. Antunes, L.M. Bettencourt and W.H. Zurek, *Phys. Rev. Lett.* **82**, 2824 (1999) [hep-ph/9811426].
 - [4] P. Laguna and W.H. Zurek, *Phys. Rev.* **D58**, 085021 (1998) [hep-ph/9711411].
 - [5] V.M.H. Ruutu *et al.*, *Nature* **382**, 334 (1996) [cond-mat/9512117]; V.M.H. Ruutu *et al.*, *Phys. Rev. Lett.* **80**, 1465 (1998) [cond-mat/9706038]; C. Bäuerle *et al.*, *Nature* **382**, 332 (1996).
 - [6] M.E. Dodd *et al.*, *Phys. Rev. Lett.* **81**, 3703 (1998).
 - [7] M.B. Hindmarsh and T.W.B. Kibble, *Rept. Prog. Phys.* **58**, 477 (1995) [hep-ph/9411342].
 - [8] S. Rudaz and A.M. Srivastava, *Mod. Phys. Lett.* **A8**, 1443 (1993) [hep-ph/9212279]; M. Hindmarsh, A. Davis and R. Brandenberger, *Phys. Rev.* **D49**, 1944 (1994) [hep-ph/9307203]; T.W.B. Kibble and A. Vilenkin, *Phys. Rev.* **D52**, 679 (1995) [hep-ph/9501266].
 - [9] A. Yates and W.H. Zurek, *Phys. Rev. Lett.* **80**, 5477 (1998) [hep-ph/9801223].
 - [10] R. Carmi and E. Polturak, *Phys. Rev.* **B60**, 7595 (1999) [cond-mat/9908244].
 - [11] R. Carmi, E. Polturak and G. Koren, *Phys. Rev. Lett.* **84**, 4966 (2000).
 - [12] M. Hindmarsh and A. Rajantie, in preparation.
 - [13] J. Ranft, J. Kripfganz and G. Ranft, *Phys. Rev.* **D28**, 360 (1983); K. Kajantie, M. Karjalainen, M. Laine, J. Peisa and A. Rajantie, *Phys. Lett.* **B428**, 334 (1998) [hep-ph/9803367].